# Deriving Global Material Properties of a Microscopically Heterogeneous Medium – Computational Homogenisation and Opportunities in Visualisation

C. B. Hirschberger[1], S. Ricker[1], P. Steinmann[2], N. Sukumar[3]

[1] University of Kaiserslautern
Chair of Applied Mechanics, Department of Mechanical and Process Engineering
P.O. Box 3049, 67653 Kaiserslautern, Germany
bhirsch@rhrk.uni-kl.de

[2] University of Erlangen-Nuremberg
Chair of Applied Mechanics, Department of Mechanical Engineering
Egerlandstraße 5, 91058 Erlangen, Germany
steinmann@ltm.uni-erlangen.de

[3] University of California, Davis
Department of Civil & Environmental Engineering
One Shields Avenue, Davis, CA 95616. U.S.A.
nsukumar@ucdavis.edu

**Abstract:** In order to derive the overall mechanical response of a microscopically material body, both the theoretical and the numerical framework of multi scale consideration coined as computational homogenisation is presented. Instead of resolving the actual heterogeneous microstructure in all detail for its simulation, representative micro elements are considered which provide the material properties for the coarse or rather scale. This procedure allows for a smaller and less inexpensive computation. However both the chance and challenge of visualising the decisive features arise on two scales.

## 1 Introduction

If a material—although it may appear macroscopically homogeneous—at a closer look possesses a heterogeneous microstructure, we would rather account for this microstructure than posing a inaccurate macroscopic constitutive assumption. Such microscopic inhomogeneities may for instance be voids, small inclusion, micro cracks [NNH99] as for instance those that occur in metal alloy systems, polymer blends, porous and cracked media, polycrystalline materials, or composites [KBB01].

Approaches to obtain the overall characteristics of such heterogeneous materials have been

developed since the 1960s by e. g. Hashin and Shtrikman, Hill, Willis and Walpole [HS62, Hil63, Hil72, Has64, Wal66, Wil77, Wil81, Has83] and are comprised in the recent monograph of Nemat-Nasser and Hori [NNH99]. They provide a framework to relate overall aggregate properties to micro-properties, thereby they involve the concept of a representative volume element (RVE) over which an averaging of key quantities is performed [NNH99]:

> An RVE for a material point of continuum mass is a material volume which is statistically representative of the infinitesimal material element.

Within the framework of computational mechanics involving multiple scales, these concepts have been applied to the numerical solution during the last decade by several researchers [TIK98, SBM98, MSS99, MMS99, THKK00, FC00, TK01, KBB01, MMS01, Kou02, KGB02, MK02, MD04]. Rather than resolving the single heterogeneities individually, they have made use of the theoretical foundations and developed algorithms which allow to obtain macroscopic material properties from underlying microstructures during the computation as these evolve under the deformation.

In this contribution, we adopt a multiscale framework within the context of large deformations. The notation is adopted along the lines of our earlier contributions [HKS06, HKS07a, HKS07b, HKS07c], whereby we now restrict ourselves to a classical continuum without additional degrees of freedom on both the macro and the micro level.

We first describe the theoretical framework (Section 2) which involves the continuum description for both the macro and the micro scale, the latter being occupied by the representative volume element, and the relations between the two scales. Then the approach to the computational homogenisation is explained (Section 3). The paper closes with numerical examples (Section 4) and a brief conclusion (Section 5).

## 2 Homogenisation

We review the theoretical framework which relates the continuum on the macro scale, for which no constitutive assumption is made, with the underlying microstructure advocated by the representative volume element. Thereby the continuum mechanical framework of finite deformation is pursued analogous to the contributions of [Hil72, KGB02, Kou02, KGB02, Mie03]. Note that throughout the paper quantities on the macro scale are denoted by $\bar{\bullet}$, while quantities within the RVE are denoted by plain letters. Body forces will be omitted on both scales.

### 2.1 Governing equations on the macro scale

As already indicated, the mechanical behaviour on the macro scale is described within a standard continuum mechanics framework, whereby no constitutive assumption is posed.

### 2.1.1 Continuum framework

On the macro level we consider the behaviour of a physical point $\bar{\mathcal{P}}$ within a body $\mathcal{B}$. It has the initial placement $\bar{\boldsymbol{X}}$ in the material configuration $\bar{\mathcal{B}}_0$ and the current placement $\bar{\boldsymbol{x}}$ in the spatial configuration $\bar{\mathcal{B}}_t$, respectively. The deformation map $\bar{\boldsymbol{\varphi}}$ and deformation gradient $\bar{\boldsymbol{F}}$ are defined as

$$\bar{\boldsymbol{x}} = \bar{\boldsymbol{\varphi}}(\bar{\boldsymbol{X}}, t) \qquad\qquad \bar{\boldsymbol{F}} = \nabla_{\bar{\boldsymbol{X}}} \bar{\boldsymbol{\varphi}} \tag{1}$$

The weak formulation of the balance of momentum, derived from the Dirichlet principle[1], reads

$$\int_{\bar{\mathcal{B}}_0} \bar{\boldsymbol{P}} : \delta \bar{\boldsymbol{F}} \mathrm{d}V = \int_{\partial \bar{\mathcal{B}}_0} \bar{\boldsymbol{t}}_0 \cdot \delta \bar{\boldsymbol{\varphi}} \mathrm{d}A \tag{2}$$

whereby $\bar{\boldsymbol{P}}$ denotes the Piola stress and $\bar{\boldsymbol{t}}_0$ the corresponding traction vector. Hereby the terms on the left represent the internal and those on the right the external virtual work, respectively. The resulting strong or rather local form of the balance of momentum and the corresponding boundary conditions read

$$\mathrm{Div}\, \bar{\boldsymbol{P}} = \boldsymbol{0} \quad \text{in } \bar{\mathcal{B}}_0 \qquad\qquad \bar{\boldsymbol{P}} \cdot \bar{\boldsymbol{N}} = \bar{\boldsymbol{t}}_0 \quad \text{on } \partial \bar{\mathcal{B}}_0 \tag{3}$$

for the considered static case. No constitutive assumption is made on the macro level, but rather obtained from the underlying micro structure.

## 2.2 Governing equations on the micro scale

The set of governing equations on the RVE level comprises both the continuum framework and a constitutive formulation.

### 2.2.1 Continuum framework

The classical continuum framework as introduced for the macro scale, is also adopted for the micro scale. Particularly, the deformation map $\boldsymbol{\varphi}$ and the deformation gradient $\boldsymbol{F}$ read

$$\boldsymbol{x} = \boldsymbol{\varphi}(\boldsymbol{X}, t) \qquad\qquad \boldsymbol{F} = \nabla_{\boldsymbol{X}} \boldsymbol{\varphi}\,. \tag{4}$$

The balance of momentum and the corresponding boundary conditions

$$\mathrm{Div}\, \boldsymbol{P} = \boldsymbol{0} \quad \text{in } \mathcal{B}_0\,, \qquad\qquad \boldsymbol{P} \cdot \boldsymbol{N} = \boldsymbol{t}_0 \quad \text{on } \partial \mathcal{B}_0 \tag{5}$$

[1]The Dirichlet principle requires the energy density to be stationary for the system to be in equilibrium, i e., $\mathrm{D}_\delta(\int_{\bar{\mathcal{B}}_0} \bar{U}_0(\bar{\boldsymbol{\varphi}}, \bar{\boldsymbol{F}}; \bar{\boldsymbol{X}}) \mathrm{d}V - \int_{\partial \bar{\mathcal{B}}_0} \bar{v}_0(\bar{\boldsymbol{\varphi}}; \bar{\boldsymbol{X}})) = 0$, whereby $\mathrm{D}_\delta$ denotes a variation with respect to all kinematic quantities at fixed material placement $\bar{\boldsymbol{X}}$. Furthermore $U_0$ denotes the total bulk energy density and $v_0$ the surface energy density.

have to be fulfilled for the RVE to be in static equilibrium. Herein $\boldsymbol{P}$ is the Piola stress within the RVE and $\boldsymbol{t}_0$ denotes the spatial traction vector on the material surface of the RVE. The weak form is stated in complete analogy to (2) as

$$\int_{\mathcal{B}_0} \boldsymbol{P} : \delta\boldsymbol{F}\mathrm{d}V = \int_{\partial\mathcal{B}_0} \boldsymbol{t}_0 \cdot \delta\boldsymbol{\varphi}\mathrm{d}A\,. \tag{6}$$

### 2.2.2 Constitutive formulation

Any suitable constitutive behaviour can be assigned with the micro level. In the present contribution for the sake of simplicity, we use a hyperelastic material which obeys the neo-Hooke formulation for the energy density

$$U_0(\boldsymbol{F};\boldsymbol{X}) = \tfrac{1}{2}[\lambda \ln^2(\det(\boldsymbol{F})) + \mu[\boldsymbol{F}:\boldsymbol{F} - n^{\dim} - 2\ln(\det(\boldsymbol{F}))]]\,, \tag{7}$$

wherein $\mu$ and $\lambda$ are the Lamé material constants and $n^{\dim}$ denotes the spatial dimension of the problem. With this formulation the Piola stress $\boldsymbol{P} := \mathsf{D}_{\boldsymbol{F}} U_0$ can be evaluated.

## 2.3 Micro-to-macro transition

The relation between a macro continuum point and the underlying microstructure is based on the averaging of the decisive quantities over the corresponding representative volume element.

### 2.3.1 Averaging of quantities over the RVE

The volume averages over the RVE of the deformation gradient, the Piola stress, and the virtual work

$$\langle\boldsymbol{F}\rangle = \frac{1}{V}\int_{\mathcal{B}_0} \boldsymbol{F}\mathrm{d}V\,, \qquad \langle\boldsymbol{P}\rangle = \frac{1}{V}\int_{\mathcal{B}_0} \boldsymbol{P}\mathrm{d}V\,, \qquad \langle\boldsymbol{P}:\delta\boldsymbol{F}\rangle = \frac{1}{V}\int_{\mathcal{B}_0} \boldsymbol{P}:\delta\boldsymbol{F}\mathrm{d}V \tag{8}$$

are recalled here and transformed to boundary integrals[2]:

$$\langle\boldsymbol{F}\rangle = \frac{1}{V}\int_{\partial\mathcal{B}_0} \boldsymbol{\varphi}\otimes\boldsymbol{N}\mathrm{d}A\,, \quad \langle\boldsymbol{P}\rangle = \frac{1}{V}\int_{\partial\mathcal{B}_0} \boldsymbol{t}_0\otimes\boldsymbol{X}\mathrm{d}A\,, \quad \langle\boldsymbol{P}:\delta\boldsymbol{F}\rangle = \frac{1}{V}\int_{\partial\mathcal{B}_0} \boldsymbol{t}_0\cdot\delta\boldsymbol{\varphi}\,\mathrm{d}A\,. \tag{9}$$

These will be related to the macroscopic quantities next.

[2]The following relations are utilised to derive the representation of the volume averages as surface integrals over the boundary:

$$\begin{aligned}
\boldsymbol{F} &= \nabla_{\boldsymbol{X}}\boldsymbol{\varphi} = \nabla_{\boldsymbol{X}}\boldsymbol{\varphi}\cdot\boldsymbol{I} + \boldsymbol{\varphi}\cdot\mathrm{Div}\,(\boldsymbol{I}) = \mathrm{Div}\,(\boldsymbol{\varphi}\otimes\boldsymbol{I})\\
\boldsymbol{P}^t &= \boldsymbol{I}\cdot\boldsymbol{P}^t + \boldsymbol{X}\otimes\mathrm{Div}\,\boldsymbol{P} = \nabla_{\boldsymbol{X}}\boldsymbol{X}\cdot\boldsymbol{P}^t + \boldsymbol{X}\otimes\mathrm{Div}\,\boldsymbol{P} = \mathrm{Div}\,(\boldsymbol{X}\otimes\boldsymbol{P})\\
\boldsymbol{P}:\delta\boldsymbol{F} &= \mathrm{Div}\,(\boldsymbol{\varphi}\cdot\boldsymbol{P}) - \mathrm{Div}\,\boldsymbol{P}\cdot\delta\boldsymbol{\varphi} = \mathrm{Div}\,(\delta\boldsymbol{\varphi}\cdot\boldsymbol{P})\,.
\end{aligned}$$

### 2.3.2 Equivalence of averages and macro quantities

It is postulated that the macroscopic deformation gradient, Piola stress and virtual work are equivalent to the averages:

$$\bar{\boldsymbol{F}} \equiv \langle \boldsymbol{F} \rangle \,, \qquad \bar{\boldsymbol{P}} \equiv \langle \boldsymbol{P} \rangle \,, \qquad \bar{\boldsymbol{P}} : \delta\bar{\boldsymbol{F}} \equiv \langle \boldsymbol{P} : \delta\boldsymbol{F} \rangle \,. \tag{10}$$

With this framework at hand, boundary conditions stemming from the macroscopic quantities are imposed on the RVE using (9), whereby the Hill condition

$$\langle \boldsymbol{P} \rangle : \langle \delta\boldsymbol{F} \rangle \doteq \langle \boldsymbol{P} : \delta\boldsymbol{F} \rangle \tag{11}$$

must be fulfilled.

### 2.3.3 Boundary conditions on the RVE imposed by macro quantities

There are three ways to apply boundary conditions on the RVE based on the macroscopic quantities, which meet the Hill condition (11): The first is referred to as *linear displacement boundary conditions*, the second as an imposition of *periodic displacements and antiperiodic tractions*. A third option is to apply *constant traction* on the boundary. While the first two options are depicted in Figure 1, we omit the latter case here for the sake of brevity. They all are based on the assumption that the origin of the coordinate system is placed in the volumetric centre of the RVE. For linear displacement boundary conditions, the displacement on the RVE boundary is a linear mapping of the reference placement by means of the macro deformation gradient:

$$\boldsymbol{\varphi} = \bar{\boldsymbol{F}} \cdot \boldsymbol{X} \quad \text{on } \partial\mathcal{B}_0 \,. \tag{12}$$

In case of periodic boundary conditions, deformations of opposite boundaries allow for periodicity, while from equilibrium the tractions on opposite edges will be antiperiodic:

$$[\boldsymbol{\varphi}^+ - \boldsymbol{\varphi}^-] = \bar{\boldsymbol{F}} \cdot [\boldsymbol{X}^+ - \boldsymbol{X}^-] \,, \qquad \boldsymbol{t}_0^+ - \boldsymbol{t}_0^- = \boldsymbol{0} \quad \text{on } \partial\mathcal{B}_0^\pm \,. \tag{13}$$

Thereby the positive and negative boundaries, $\mathcal{B}_0^+$ and $\mathcal{B}_0^-$, respectively, are located on opposite edges of the RVE.

## 3 Computational Homogenisation

The homogenisation concept introduced previously is embedded into a nonlinear finite element framework. Particularly, the macro specimen is discretised by a finite element mesh. During the simulation of a boundary value problem, at each elemental integration point of each element, the material properties are evaluated by means of an underlying RVE along the lines of the contributions by Miehe, Geers, and others [MSS99, FC00, KBB01, KGB02]. Due to the geometrically and physically nonlinear framework, this multi-scale computation requires an iterative solution procedure on both the macro and the micro level, as we illustrate in the simplified flowchart of Figure 2.

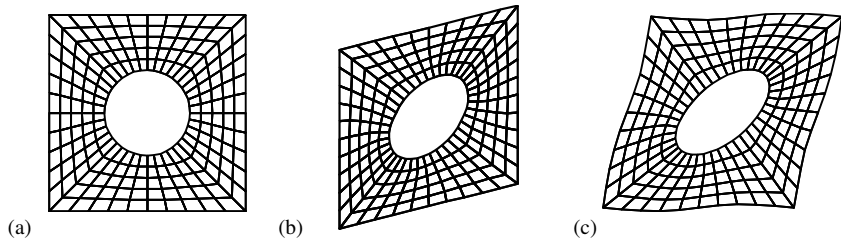


Figure 1: Representative volume elements: (a) undeformed mesh and deformed mesh under (b) linear displacement on the boundary, (c) periodic displacement on the boundary.

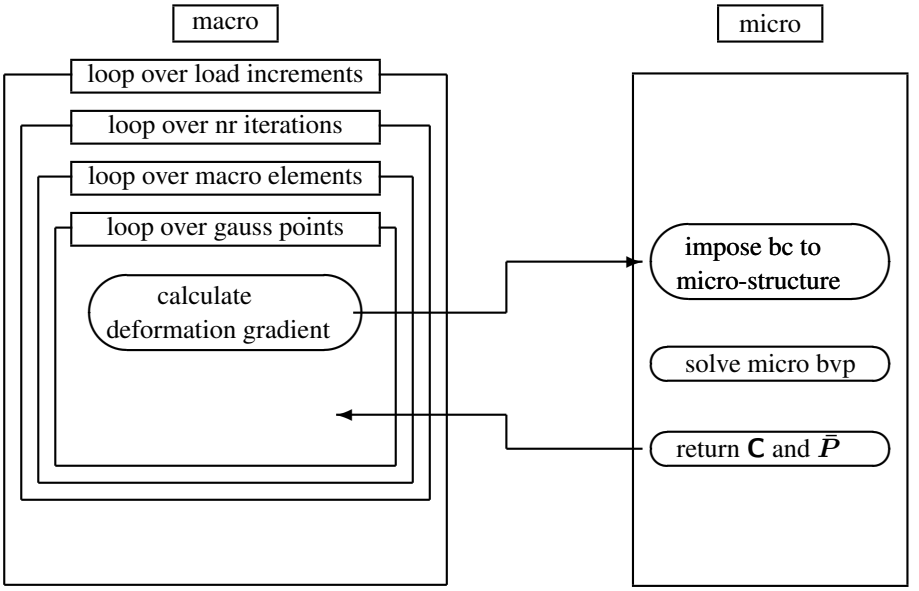


Figure 2: Simplified flow chart of computational micro–macro transition.

### 3.1 Application of the boundary conditions on the RVE

According to Section 2.3.3, different types of boundary conditions can be applied onto the RVE within the stepwise and iterative numerical evaluation of the particular RVE at a macroscopic integration point. In case of linear displacement on the boundary, the displacements of all boundary nodes are prescribed as shown in Figure 1(b). For the periodic case, only the displacement of three independent corner nodes are prescribed, see Figure 1(c).

### 3.2 Solution of the nonlinear system of equations of the RVE

With the respective boundary conditions, the micro system of equations is solved. In the case of fully prescribed boundary displacement, this is straightforward. With the displacement boundary condition stemming from the current increment of the macro deformation gradient, an iteration scheme (e. g. Newton-Raphson) is used to find the solution at (micro) equilibrium.

The linearised system of equations with the algorithmic tangent tensor $\mathbf{K}_{IK}$

$$\mathbf{K}_{IK} \cdot \Delta\boldsymbol{\varphi}_K = \boldsymbol{f}_I^{\text{ext}} - \boldsymbol{f}_I^{\text{int}}\,, \qquad \mathbf{K}_{IK} = \frac{\partial \mathbf{R}_I}{\partial \boldsymbol{\varphi}_{\text{K}}} \tag{14}$$

is solved such that the residual vector becomes zero:

$$\mathbf{R}_I = \mathop{\mathbf{A}}_{e=1}^{n_{\text{el}}} \int_{\mathcal{B}_0} \boldsymbol{P} \cdot \nabla_{\boldsymbol{X}} N_I - \boldsymbol{f}_I^{\text{ext}} \stackrel{!}{=} \mathbf{0}\,. \tag{15}$$

Note that for periodic displacement and anti-periodic traction on the boundary, the periodicity constraints must be imposed before the solution of the system is performed. We transform the system (14) towards a new system only formulated in terms of independent degrees of freedom

$$\mathbf{K}^\star \cdot \Delta\boldsymbol{\varphi}_i = \Delta\boldsymbol{f}^\star \tag{16}$$

as proposed by [Kou02]. Thereby the transformed stiffness matrix and the transformed incremental load vector read:

$$\mathbf{K}^\star = \mathbf{K}_{\text{ii}} + \mathbf{C}_{\text{di}}^{\text{t}} \cdot \mathbf{K}_{\text{id}} + \mathbf{K}_{\text{id}} \cdot \mathbf{C}_{\text{di}} + \mathbf{C}_{\text{di}}^{\text{t}} \cdot \mathbf{K}_{\text{dd}} \cdot \mathbf{C}_{\text{di}} \tag{17}$$

$$\Delta\boldsymbol{f}^\star = \Delta\boldsymbol{f}_{\text{i}} + \mathbf{C}_{\text{di}}^{\text{t}} \cdot \Delta\boldsymbol{f}_{\text{d}}\,, \tag{18}$$

which is based on the relation $\Delta\boldsymbol{\varphi}_{\text{d}} = \mathbf{C}_{\text{di}} \cdot \Delta\boldsymbol{\varphi}_{\text{i}}$ between the dependent and the independent degrees of freedom with the so-called dependency matrix $\mathbf{C}_{\text{di}}$.

### 3.3 Obtaining the macro stress and tangent operator

Once the solution has been obtained iteratively, the macroscopic stress and tangent operator are computed. With the equivalence $(10)_2$ the macro Piola stress $\bar{\boldsymbol{P}}$ is discretely evaluated as a summation over boundary nodes:

$$\Delta\bar{\boldsymbol{P}} = \frac{1}{V}\sum_I \Delta\boldsymbol{f}_I \otimes \boldsymbol{X}_I \,. \tag{19}$$

With (14), the tangent operator in the relation $\Delta\bar{\boldsymbol{P}} = \partial_{\bar{\boldsymbol{F}}}\bar{\boldsymbol{P}} : \Delta\bar{\boldsymbol{F}}$ is extracted as[3]

$$\bar{\mathsf{A}} := \partial_{\bar{\boldsymbol{F}}}\bar{\boldsymbol{P}} = \frac{1}{V}\sum_I\sum_K \mathsf{K}_{IK}\,\overline{\otimes}\,[\boldsymbol{X}_K \otimes \boldsymbol{X}_I] \,. \tag{20}$$

In the case of linear displacement boundary conditions, the summations over nodes (I) and (K) run over all boundary nodes, while for periodic boundary conditions, only the three independent boundary nodes are taken into account. In each of these cases a condensation is applied to the stiffness matrix at the solved state.

## 4 Numerical examples and visualisation

Based on the presented framework, some numerical examples are shown.

Figure 3 shows a benchmark-type problem. Hereby, the macro specimen is discretised with four finite elements, each of which possesses four integration points, which are depicted by the bullets. At each integration point an underlying RVE with a circular centered hole shown in Figure $1(a)$ is installed. Uniaxial loading is applied on the macro structure. The influence of different choices for the RVE boundary conditions (Section 3.1) on the macro response are examined. Thereby, the macroscopic load displacement curves reflect the fact that the RVE under displacement boundary conditions exhibits a stiffer behaviour than the RVE under periodic boundary conditions.

As a more realistic example, Figure 4 shows a rectangular specimen under uniaxial tension, the response of which is determined with the same underlying RVE, in particular a quadratic specimen which has a circular centered hole in the undeformed configuration. On the deformed macro mesh the Cauchy stress component $\bar{\sigma}_{22}$ is plotted. Furthermore, at four several placements of the macro specimen the deformed underlying micro structures are scaled into. Both the deformed shape and the distribution of the longitudinal normal component of the Cauchy stress, $\sigma_{22}$, strongly vary depending on the position at which the RVE is evaluated. Contrary to our last contribution [HKS06], here the Cauchy stress is a symmetric quantity due to the used standard continuum .

[3] The modified dyadic product of two second-order tensors is defined as $[\boldsymbol{A}\,\overline{\otimes}\,\boldsymbol{B}] : \boldsymbol{C} = \boldsymbol{A}\cdot\boldsymbol{C}\cdot\boldsymbol{B}^{\mathrm{t}}$.

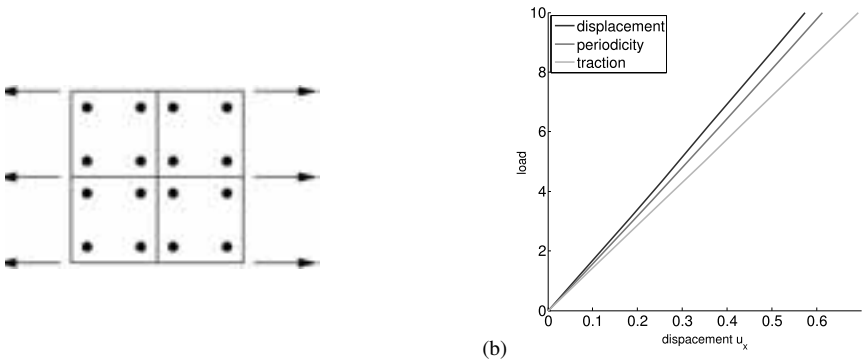


(a) (b)

Figure 3: (a) Macro boundary value problem discretised with four elements with four integration points per element. (b) Comparison of macro load displacement curves for different RVE boundary conditions (reproduced in colorplate 193).

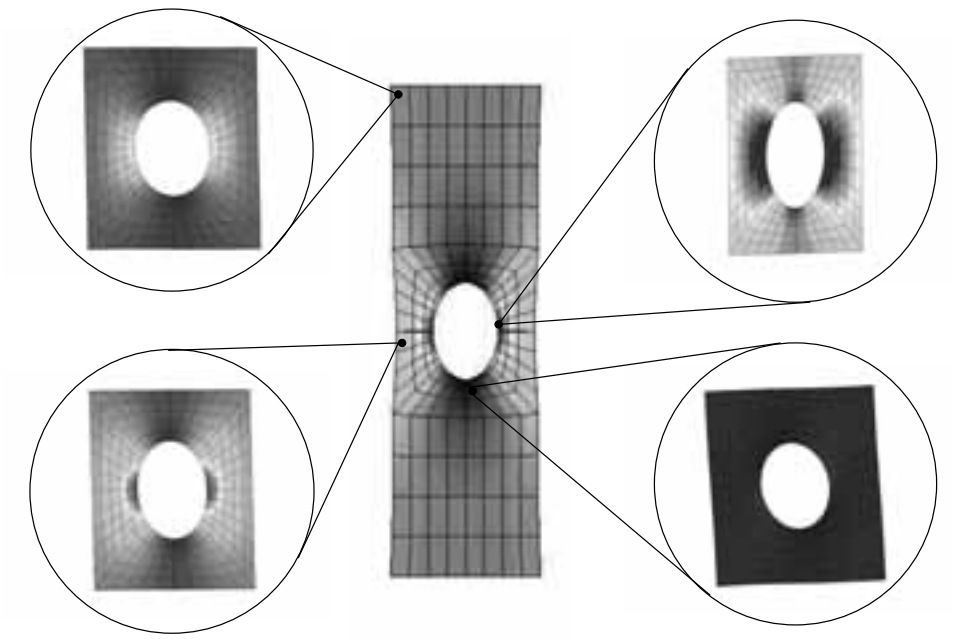

Figure 4: Deformed specimen with circular hole under longitudinal tension and deformed RVEs with logitudinal normal stress component $\bar{\sigma}_{22}$ and $\sigma_{22}$, respectively (reproduced in colorplate 193).

## 5 Conclusion

In this contribution, we have given a briew review on a finite-element-based multi scale method coined as computational homogenisation or rather $FE^2$. This approach is characterised by the solution of separate boundary value problems on both the macro and the

micro scale, which are linked at each integration point of each macro finite element, while the material behaviour is exclusively determined by the constitution and response of the micro structure.

While here we have chosen a continuous RVE with a phenomenological constitutive behaviour, one could also employ other material laws or other compositions. For instance inelastic formulations of standard continua [RMS07] or micromorphic continua [HS07] represent a significant challenge. A further extension of the methodology to obtain material properties of cohesive layers has recently been developed by the authors [HRSS07, HRSS08, HSS08]. In the contribution of [HSS08] a micromorphic continuum [HKS06, HKS07b], was employed at the micro level to account for a large intrinsic substructure underlying to the material layer. Thereby nonsymmetric stress measures as well as higher order tensors evolve, which from our perspective represent further challenges in the visualisation. Futhermore we would like to refer to the discrete element method which accounts for the interaction of single particles [MKS06, MKS07, MSK07], or atomistic models [SS03, SES07] and, if employed at the microstructural scale, can lead to realistic simulation of structures at the nano level.

## Acknowledgement

We gratefully acknowledge financial support by the German Science Foundation (DFG) within the International Research Training Group 1131 "Visualization of Large and Unstructured Data Sets – Applications in Geospatial Planning, Modeling, and Engineering" as well as through the Research Training Group 814 "Engineering Materials on Different Scales – Experiment, Modelling, and Simulation".

## References

[FC00] F. Feyel and J.-L. Chaboche. $FE^2$ multiscale approach for modelling the elastoviscoplastic behaviour of long fibre SiC/Ti composites materials. *Comput. Methods Appl. Mech. Engrg.*, 183:309–330, 2000.

[Has64] Z. Hashin. Theory of mechanical behaviour of heterogeneous media. *Appl. Mech. Rev.*, 17:1–9, 1964.

[Has83] Z. Hashin. Analysis of composite materials – A survey. *J. Appl. Mech.*, 50:481–505, 1983.

[Hil63] R. Hill. Elastic properties of reinforced solids: Some theoretical principles. *J. Mech. Phys. Solid.*, 11:357–372, 1963.

[Hil72] R. Hill. On constitutive macro-variables for heterogeneous solids at finite strain. *Proc. Roy. Soc. Lond. A*, 326:131–147, 1972.

[HKS06] C. B. Hirschberger, E. Kuhl, and P. Steinmann. Computational modelling of micromorphic continua – theory, numerics, and visualisation challenges. In H. Hagen, A. Kerren,

and P. Dannenmann, editors, *Visualization of large and unstructured data sets*, volume S-4 of *GI-Edition Lecture Notes in Informatics (LNI)*, pages 155–164, 2006.

[HKS07a] C. B. Hirschberger, E. Kuhl, and P. Steinmann. Computational material forces in micromorphic continua. *Proc. Appl. Math. Mech.*, 6:379–380, 2007.

[HKS07b] C. B. Hirschberger, E. Kuhl, and P. Steinmann. On deformational and configurational mechanics of micromorphic hyperelasticity – theory and computation. *Comput. Methods Appl. Mech. Engrg.*, 196:4027–4044, 2007.

[HKS07c] C. B. Hirschberger, E. Kuhl, and P. Steinmann. Recent aspects in the mechanics of micromorphic continua. In *Proceedings of the International Workshop on Nonlocal Modeling of Materials Failure, Wuppertal*, pages 3–14. Aedificatio Publishers, 2007.

[HRSS07] C. B. Hirschberger, S. Ricker, P. Steinmann, and N. Sukumar. A computational homogenisation approach for cohesive interfaces. In D. R. J. Owen and E. O nate, editors, *Computational Plasticity IX: Fundamentals and Applications*, pages 442–445. CIMNE, 2007.

[HRSS08] C. B. Hirschberger, S. Ricker, P. Steinmann, and N. Sukumar. On the computational homogenization of a heterogeneous material layer. *Eng. Fract. Mech.*, submitted, 2008.

[HS62] Z. Hashin and S. Shtrikman. On some variational principles in anisotropic and nonhomogeneous elasticity. *J. Mech. Phys. Solid.*, 10:335–342, 1962.

[HS07] C. B. Hirschberger and P. Steinmann. Classification of concepts in thermodynamically consistent generalized plasticity. *J. Engineering Mech.*, submitted, 2007.

[HSS08] C. B. Hirschberger, N. Sukumar, and P. Steinmann. Computational homogenization of material layers with micromorphic mesostructure. *Phil. Mag.*, submitted, 2008.

[KBB01] V. G. Kouznetsova, W. A. M. Brekelmans, and F. P. T. Baaijens. An approach to micro-macro modeling of heterogeneous materials. *Comput. Mech.*, 27:37–48, 2001.

[KGB02] V. G. Kouznetsova, M. G. D. Geers, and W. A. M. Brekelmans. Multi-scale constitutive modelling of heterogeneous materials with a gradient-enhanced computational homogenization scheme. *Int. J. Numer. Meth. Engng*, 54:1235–1260, 2002.

[Kou02] V. G. Kouznetsova. *Computational Homogenization for the Multiscale Analysis of Multi-Phase Materials*. PhD thesis, Technische Universiteit Eindhoven, 2002.

[MD04] C. Miehe and J. Dettmar. A framework for micro-to-macro transitions in periodic particle aggregates of granular materials. *Comput. Methods Appl. Mech. Engrg.*, 193:225–256, 2004.

[Mie03] C. Miehe. Computational micro-to-macro transitions discretized micro-structures of heterogeneous materials at finite strains based on the minimization of averaged incremental energy. *Comput. Methods Appl. Mech. Engrg.*, 192:559–591, 2003.

[MK02] C. Miehe and A. Koch. Computational micro-to-macro transitions of discretized microstructures undergoing small strains. *Arch. Appl. Mech.*, 72:300–317, 2002.

[MKS06] H. A. Meier, E. Kuhl, and P. Steinmann. On discrete modeling and visualization of granular media. In H. Hagen, A. Kerren, and P. Dannenmann, editors, *Visualization of Large and Unstructured Data Sets*, volume S-4, pages 165–175. Lecture Notes in Informatics, 2006.

[MKS07] H. A. Meier, E. Kuhl, and P. Steinmann. A note on the generation of periodic granular microstructures based on grain size distributions. *Int. J. Numer. Anal. Meth. Geomech.*, 2007. in press.

[MMS99] J. C. Michel, H. Moulinec, and P. Suquet. Effective properties of composite materials with periodic microstructure: a computational approach. *Comput. Methods Appl. Mech. Engrg.*, 172:109–143, 1999.

[MMS01] J. C. Michel, H. Moulinec, and P. Suquet. A computational scheme for linear and non-linear composites with arbitrary phase contrast. *Int. J. Numer. Meth. Engng*, 52:139–160, 2001.

[MSK07] H. A. Meier, P. Steinmann, and E. Kuhl. Towards multiscale computation of confined granular media – contact forces, stresses and tangent operators. *Technische Mechanik*, 2007. submitted.

[MSS99] C. Miehe, J. Schotte, and J. Schröder. Computational micro-macro transitions and overall moduli in the analysis of polycrystals at large strains. *Comput. Mater. Sci.*, 16:372–382, 1999.

[NNH99] A. Nemat-Nasser and M. Hori. *Micromechanics: Overall Properties of Heterogeneous Materials*. North-Holland Elsevier, 2nd revised edition, 1999.

[RMS07] S. Ricker, A. Menzel, and P. Steinmann. Computational homogenization for discrete micro-structures including damage. In M. Jirásek, Z. Bittnar, and H. Mang, editors, *Modelling of Heterogeneous Materials*, pages 182–183, Prague, 2007.

[SBM98] R. J. M. Smit, W. A. M. Brekelmans, and H. E. H. Meijer. Prediction of the mechanical behaviour of nonlinear heterogeneous systems by multi-level finite element modeling. *Comput. Methods Appl. Mech. Engrg.*, 155:181–192, 1998.

[SES07] P. Steinmann, A. Elizondo, and R. Sunyk. Studies of validity of the Cauchy-Born rule by direct comparison of continuum and atomistic modelling. *Modelling Simul. Mater. Sci. Eng.*, 15:S271–S281, 2007.

[SS03] R. Sunyk and P. Steinmann. On higher gradients in continuum-atomistic modelling. *Int. J. Solid Struct.*, 40:6877–6896, 2003.

[THKK00] K. Terada, M. Hori, T. Kyoya, and N. Kikuchi. Simulation of the multi-scale convergence in computational homogenzation approaches. *Int. J. Solid Struct.*, 37:2285–2311, 2000.

[TIK98] K. Terada, T. Ito, and N. Kikuchi. Characterization of the mechanical behaviors of solid-fluid mixture by the homogenization method. *Comput. Methods Appl. Mech. Engrg.*, 153:233–257, 1998.

[TK01] K. Terada and N. Kikuchi. A class of general algorithms for multi-scale analyses of heterogeneous media. *Comput. Methods Appl. Mech. Engrg.*, 190:5427–5464, 2001.

[Wal66] L. J. Walpole. On bounds for the overall elastic moduli of inhomogeneous systems – I. *J. Mech. Phys. Solid.*, 14:151–162, 1966.

[Wil77] J. R. Willis. Bounds and self-consistent estimates for the overall properties of composites. *J. Mech. Phys. Solid.*, 25:185–202, 1977.

[Wil81] J. R. Willis. Variational and related methods for the overall properties of anisotropic composites. *Adv. Appl. Mech.*, 21:1–78, 1981.